

See discussions, stats, and author profiles for this publication at: <https://www.researchgate.net/publication/7332741>

Cycloviolacin H₄, a Hydrophobic Cyclotide from *Viola hederaceae*

ARTICLE *in* JOURNAL OF NATURAL PRODUCTS · FEBRUARY 2006

Impact Factor: 3.8 · DOI: 10.1021/np050317i · Source: PubMed

CITATIONS

38

READS

22

4 AUTHORS, INCLUDING:



Michelle L Colgrave

The Commonwealth Scientific and Industrial ...

94 PUBLICATIONS 2,495 CITATIONS

SEE PROFILE

Cycloviolacin H4, a Hydrophobic Cyclotide from *Viola hederaceae*

Bin Chen,^{†,‡} Michelle L. Colgrave,[†] Conan Wang,[†] and David J. Craik^{*,†}

Institute for Molecular Bioscience, Australian Research Council Special Research Centre for Functional and Applied Genomics, University of Queensland, Brisbane, QLD 4072, Australia, and Centre for Natural Products, Chengdu Institute of Biology, Chinese Academy of Sciences, Chengdu 610041, People's Republic of China

Received August 26, 2005

Cycloviolacin H4, a new macrocyclic miniprotein comprising 30 amino acid residues, was isolated from the underground parts of the Australian native violet *Viola hederaceae*. Its sequence, cyclo-(CAESCVWIPCTVTALLGCSCSNNVC-YNGIP), was determined by nanospray tandem mass spectrometry and quantitative amino acid analysis. A knotted disulfide arrangement, which was designated as a cyclic cystine knot motif and characteristic to all known cyclotides, is proposed for stabilizing the molecular structure and folding. The cyclotide is classified in the bracelet subfamily of cyclotides due to the absence of a *cis*-Pro peptide bond in the circular peptide backbone. A model of its three-dimensional structure was derived based on the template of the homologous cyclotide vhr1 (Trabi et al. *Plant Cell* **2004**, *16*, 2204–2216). Cycloviolacin H4 exhibits the most potent hemolytic activity in cyclotides reported so far, and this activity correlates with the size of a surface-exposed hydrophobic patch. This work has thus provided insight into the factors that modulate the cytotoxic properties of cyclotides.

Cyclotides are a recently discovered large family of macrocyclic knotted proteins that have the unique characteristics of three knotted disulfide bonds and a head-to-tail cyclized backbone and show exceptional resistance against chemical, thermal, and proteolytic degradation.¹ They are miniproteins, about 28–37 amino acid residues in length, but have well-defined secondary structures and adopt a compact three-dimensional fold in the same way as large proteins normally do.^{2–7} The cyclotides display a diverse range of biological activities, including uterotonic,⁸ HIV inhibitory,^{7,9,10} antimicrobial,¹¹ cytotoxic,¹² neurotensin antagonistic,¹³ hemolytic,¹⁴ trypsin inhibitory,¹⁵ and insecticidal activities.^{16,17} In addition to antimicrobial activity, some cyclotides such as kalata B1 and B2 have been shown to inhibit the growth and development of *Helicoverpa punctigera* and *H. armigera* larvae, suggesting that they play important roles in plant defense.^{16,17} This is supported by the recent finding of the up-regulation of cyclotide-like genes following fungal infection in maize.¹⁸ These diverse bioactivities, together with their unique structural features, make the cyclotides important in terms of potential agrochemical or pharmaceutical applications.

Cyclotides are present in plants from the Rubiaceae, Violaceae, and Cucurbitaceae families, of which the Violaceae is unique in that the cyclotides are present in all species of this family investigated so far and are extraordinarily abundant in the genus *Viola*.^{19,20} The genus *Viola* consists of 500 species worldwide, of which *V. hederaceae* is native to Australia and known as the “Australian violet”. Recent studies resulted in the discovery that more than 60 different cyclotides are expressed in this plant; the amino acid sequence of six new cyclotides and the solution structures of two tissue-specific cyclotides were determined.^{6,7,21} Vhl-1, one of the leaf-specific cyclotides, showed anti-HIV activity, making it an attractive molecular template to design more potent analogues for medical applications.⁷ In the current study, we report the results of investigation of a new cyclotide, distinguished by its highly hydrophobic nature, from this plant. Cycloviolacin H4 is unique in being the only cyclotide discovered so far that does not contain any positively charged residues.

Results and Discussion

In our previous studies, six new cyclotides were isolated from different parts of *V. hederaceae* and their sequences characterized

as shown in Table 1. We observed that cyclotide expression patterns varied in different parts of the plant and that some cyclotides, such as kalata B1, are present in all plant parts, while others are tissue-specifically expressed. In this study, we focused on characterization of the most hydrophobic cyclotide, designated as cycloviolacin H4, which is present only in underground parts of the plant, including roots, bulbs, and underground runners. We separated these three parts of *V. hederaceae* from others, homogenized the plant material in MeOH, and extracted overnight in a mixture of MeOH/CH₂Cl₂ (1:1). The procedure included the addition of H₂O to remove the CH₂Cl₂ layer from the MeOH/H₂O fraction, evaporation of MeOH from the solution under reduced pressure, fractionation using a C18 flash column, and further separation and purification of crude cyclotides by using RP-HPLC columns. Figure 1 shows the HPLC profiles of the crude cyclotides of the plant material and the purified cycloviolacin H4. The yield of the cyclotide was ~60 µg/kg fresh plant material.

We employed a method summarized as Method A in Figure 2, which proved to be efficient in sequencing other cyclotides, to characterize the amino acid sequence of the new hydrophobic cyclotide. The native peptide was reduced by TCEP, with the reduction of the cyclotide confirmed by the presence of peaks at *m/z* 1034.7³⁺ and 776.3⁴⁺, which correspond to a molecular mass of 3101 Da. The failure of the reduced peptide to be digested by trypsin indicated that it does not contain any basic amino acids such as Arg or Lys residues, which is unusual because at least one of these two residues exists in all known cyclotides.²¹ Amino acid analysis (Table 2) of the cyclotide confirmed this conclusion. Enzymatic digestion of the reduced peptide with a combination of trypsin and EndoGluC gave rise to peaks at *m/z* 1040.7³⁺ and 780.8⁴⁺, corresponding to a linear derivative with a molecular mass of 3119 Da due to the addition of a H₂O molecule (18 Da) across a peptide bond in the reduced peptide, suggesting the presence of one glutamic acid residue in the primary structure.

The EndoGluC digested linear peptide was difficult to analyze because it was too large to allow complete sequence determination by tandem mass spectrometry (MS/MS) fragmentation. Therefore, another strategy called “loop sequencing”¹⁹ as shown in Figure 2, Method C, was used to determine the primary structure of the cyclotide. After reduction by DTT, the reduced peptide was subjected to bromoethylamine alkylation. Each reduced and S-aminoethylated cysteine causes an increment of molecular mass of 44 Da. MS analysis of the native (3095 Da), the reduced (3101

* Corresponding author. Tel: 61-7-33462019. Fax: 61-7-33462029. E-mail: d.craik@imb.uq.edu.au.

[†] University of Queensland.

[‡] Chinese Academy of Sciences.

Table 1. Cyclotides Characterized in *V. hederaceae*^a

	loop 1	loop 2	loop 3	loop 4	loop 5	loop 6	Mass	Ref.
Möbius								
vhl-2	C G E T	C F T G T	C Y T . . . N G	C T C	D P W P V	C T R N G L . P V	3172.58	Chen, et al. 2005
cycloviolacin H3	C G E T	C F G G T	C N T . . . P G	C I C	D P W P V	C T R N G L . P V	3075.28	Chen, et al. 2005
Bracelet								
cycloviolacin H1	C G E S	C V Y I P	C L T S A . I G	C S C	. K S K V	C Y R N G . I P .	3114.72	Craik, et al. 1999
vhr1	C A E S	C V W I P	C T V T A L L G	C S C	. S N K V	C Y . N G . I P .	3109.39	Trabi, et al. 2004
cycloviolacin H2	C G E S	C V Y I P	C F . . . I P G	C S C	. R N R V	C Y L N S A I A .	3116.70	Chen, et al. 2005
vhl-1	C G E S	C A M I S F	C F T E V I . G	C S C	. K N K V	C Y L N S . I S .	3330.61	Chen, et al. 2005
cycloviolacin H4	C A E S	C V W I P	C T V T A L L G	C S C	. S N N V	C Y . N G . I P .	3095.34	this work

^a Conserved cysteine residues are boxed and presented in bold. All masses are provided as mono-isotopic mass.

Da), and the S-aminoethylated peptide (3359 Da) indicated that six cysteines are present in three intramolecular disulfide bonds. The S-aminoethylated cyclotide was isolated and purified to homogeneity by RP-HPLC (as shown in Figure 1C), which was cleaved by trypsin to yield a mixture of fragments shown in Figure 2. These fragments were then subjected to MS/MS fragmentation to allow its primary structure to be partially determined.

Fragment 1 was chosen as an example to illustrate this process, as shown in Figure 3. Complete sets of b- and y-ions were observed, allowing unambiguous determination of the sequence as VWIPC*, where the asterisk indicates that the cysteine is alkylated. The mass difference between the y₄ and y₃ ions is 186 Da, indicating the presence of a tryptophan residue. Amino acid analysis does not detect the presence of tryptophan or cysteine residues, as they are degraded during the procedure. Twenty-three amino acid residues were detected by amino acid analysis and combined with the six Cys and single Trp give a total of 30 residues. The trypsin digest of the aminoethylated peptide resulted in three major fragments: VWIPC*, TVTALLGC*, and SNNVC*YNGIPC*AESC* covering 28 of the possible 30 residues of the peptide. The remaining two residues from the highly conserved loop 4 of the cyclotide are postulated to be SC*, which fits with both the amino acid analysis data and the mass of the cyclotide. The complete list of sequence ions used to determine the sequence of cycloviolacin H4 is given in Table 3.

The loop sequencing approach was supplemented by an alternative method of cleaving the peptide backbone at multiple points. Thermolysin digestion of the TCEP reduced peptide was thus undertaken, as shown in Figure 2, Method B, to confirm the sequence as determined by trypsin digestion of the aminoethylated peptide. Fragment 6, together with fragment 3 and the two residues SC deduced from the highly conserved loop 4 of known cyclotides, unambiguously demonstrated the primary structure of cycloviolacin H4 to be cyclo-SNNVCYNGIPCAESCVWIPCTVTALLGCSC. Amino acid analysis of the peptide showed the presence of two Leu and two Ile residues within the sequence. MS/MS analysis could not distinguish between these two isobaric residues. The positions of these residues within the primary structure were initially proposed by sequence homology within the bracelet subfamily. A chymotrypsin digest (which cleaves after Leu but not Ile) was then undertaken, producing the fragments GCSCSNNVCY and LGCSCSNNVCY, thus confirming the position of these residues. Despite

the fact that it is the first example not to contain any basic amino acids, comparison of the sequence with those of known cyclotides indicated that the peptide shows high homology with them, especially with the root-derived cyclotide vhr1.⁶ Cycloviolacin H4 displays only one residue difference in loop 5 from vhr1, which is marked as peak 1 in Figure 1A and was characterized recently, as shown in Table 1.⁶ The disulfide connectivity pattern was thus proposed as shown in Figure 2 as a knotted arrangement shared by all known cyclotides. The new cyclotide falls within the bracelet subfamily on the basis of the absence of a *cis*-Pro peptide bond in loop 5 in the circular peptide backbone.

The peptide was tested for biological activity and exhibits the most potent hemolytic activity in cyclotides screened so far, as shown in Figure 4. The known hemolytic peptide melittin was used as a positive control and for comparison of the absolute levels of hemolysis under the conditions studied.²² To understand the basis for the highly hemolytic nature of cycloviolacin H4, a three-dimensional model was constructed. The high sequence identity between the root-derived cyclotide vhr1 (PDB ID 1VB8)⁶ and cycloviolacin H4 indicated that vhr1 is the most appropriate template for the homology modeling of the hydrophobic cyclotide. Ramachandran plot analysis using PROCHECK²³ reveals that 88% of the residues of the selected model molecule lie in the most favored regions, 12% lie in the additionally allowed regions, and none lie in the disallowed regions. The secondary structures visualized using MOLMOL²⁴ showed an antiparallel β -sheet linked by a turn and a short helix, which are in agreement with the reported structural data of vhr1.⁶

It appears that the membrane-disrupting activity of cyclotides on human erythrocytes is strongly correlated to their hydrophobicity. Figure 5 compares the surface representation of cycloviolacin H4 against three other cyclotides that possess varying hemolytic activities. Kalata B1, a prototypic Möbius cyclotide, and circulin A, a prototypic bracelet cyclotide, display lower hemolytic activities¹¹ than cycloviolacin H4, while tricyclon A²⁵ has the lowest hemolytic activity in naturally occurring cyclotides discovered so far. Figure 5 shows that cycloviolacin H4 has the most hydrophobic surface with 67.8% of its total surface area being hydrophobic (Table 4) and only 1.6% being charged. On the other hand, tricyclon A is the most hydrophilic, with charged and polar residues accounting for 42.4% of its surface area. Several studies have suggested that peptide-lipid interactions leading to membrane

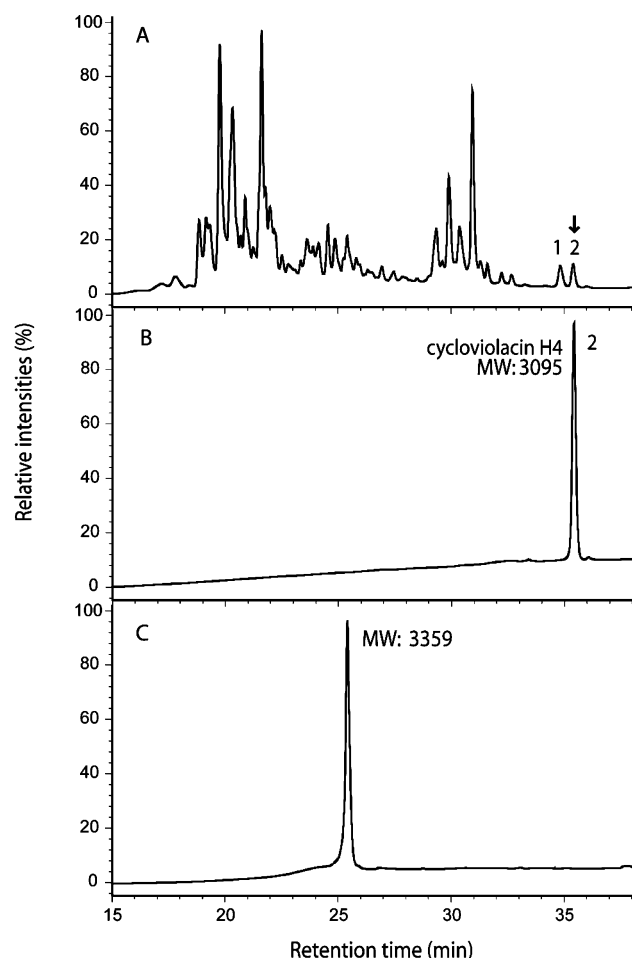


Figure 1. Purification of cycloviolacin H4. (A) RP-HPLC profile of crude cyclotide extracts from below-ground runners, bulbs, and roots of *V. hederaceae*. 5 mg/mL solutions of crude cyclotides from the three plant parts were analyzed on an analytical C-18 Grom column (150 × 2 mm, 3 μm; flow rate: 300 μL/min) with a linear acetonitrile gradient (10 to 80%) of buffer B (90% acetonitrile, 0.05% TFA) in 40 min. (B and C) The purity of cycloviolacin H4 and its S-aminoethylated derivative was assessed by RP-HPLC on the same C-18 column using the same method.

permeation play an important role in the activities of bioactive peptides.²⁶ The hydrophobic properties of cyclotides allow them to effectively approach target membranes and facilitate their interactions with lipids. The discovery of the highly hydrophobic cyclotide reported here should facilitate an understanding of the mechanisms of membrane disruption of cyclotides.

Cyclotides have been proposed as potential templates onto which pharmaceutically important peptide epitopes could be grafted.²⁷ From a clinical perspective hemolytic activity in human patients is of course an undesirable property. Therefore knowledge of the factors that modulate this activity will be important in choosing the best cyclotide analogue for such grafting studies.

Experimental Section

General Experimental Procedures. HPLC was carried out on an Agilent 1100 series system with a UV detector at variable wavelengths 215, 254, and 280 nm. Masses were analyzed on a Micromass LCT mass spectrometer equipped with an electrospray ionization source. For MALDI-TOF-MS analysis, the instrument used was a Voyager DE-STR mass spectrometer (Applied Biosystems); 200 shots per spectra were acquired in positive ion reflector mode. The laser intensity was set to 2300, the accelerating voltage to 20 000 V, and the grid voltage to 64% of the accelerating voltage; the delay time was 165 ns. The low mass gate was set to 500 Da. Data were collected between 500

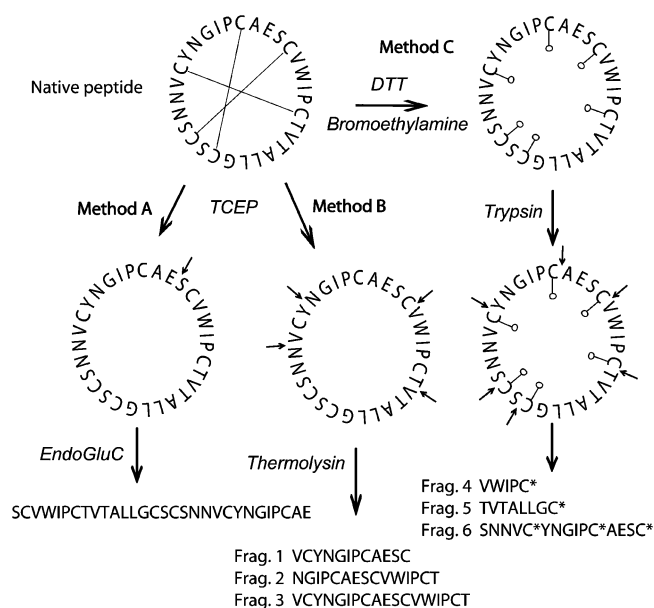


Figure 2. Methods used for amino acid sequence analysis. Sequencing Method A: cycloviolacin H4 was reduced by TCEP and subject to enzymatic digestion by trypsin or a combination of trypsin and EndoGluC. Sequencing Method B: cycloviolacin H4 was reduced by TCEP and subject to enzymatic digestion with thermolysin without alkylation. Sequencing Method C: the native peptide was reduced by DTT and alkylated by bromoethylation, then digested by trypsin.

Table 2. Amino Acid Composition Analysis of Cycloviolacin H4

amino acid	mole %	residues/mol	
		experimental ^a	theoretical
Asp+Asn	15.7	3.3	3
Ser	11.8	2.4 ^b	3
Glu+Gln	5.7	1.2	1
Gly	8.6	1.8	2
His	not detected		0
Arg	not detected		0
Thr	8.4	1.7	2
Ala	9.3	1.9	2
Pro	8.2	1.7	2
Tyr	4.7	1.0	1
Val	10.3	2.1 ^b	3
Met	not detected		0
Lys	not detected		0
Iso	8.3	1.7	2
Leu	9.0	1.9	2
Phe	not detected		0
Cys	ND ^c	ND	6
Trp	ND	ND	1

^a Normalized to an average value (A, D, E, G, L, N, and Q) of ~4.83 mol %/residue. ^b Ser and Val residues are well known to be underestimated in amino acid analyses because of degradation processes.²⁹

^c ND: Not determined.

and 5000 Da. Calibration was undertaken using a peptide mixture obtained from Sigma Aldrich (MSCal1). Nanospray MS/MS analysis was conducted on a QStar mass spectrometer, a capillary voltage of 900 V was applied, and spectra were acquired between *m/z* 60–2000 for both TOF spectra and product ion spectra. The collision energy for peptide fragmentation was varied between 10 and 50 V, depending on the size and charge of the ion. The Analyst software program was used for data acquisition and processing.

Plant Material. Fresh whole plant of *V. hederaceae* was collected at University of Queensland in Brisbane, Australia, in May 2005, and roots, bulbs, and below-ground runners were separated from other parts of the plant. The sample was authenticated by D. Craik based on a previous study.⁷ A voucher sample is held at the Institute for Molecular Bioscience, University of Queensland.

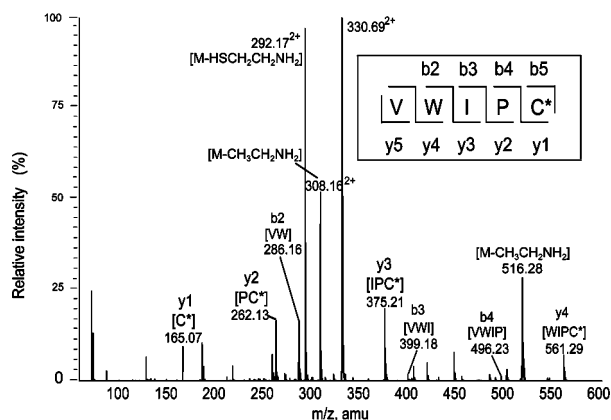


Figure 3. MS/MS fragmentation of tryptic digestion fragment 1 recorded by nanospray MS/MS spectrometry.

Isolation and Purification of Cycloviolacin H4. Fresh plant material was homogenized using a blender (Moulinex) and extracted with $\text{CH}_2\text{Cl}_2/\text{MeOH}$ (1:1) overnight. Plant debris was removed using a cotton plug. The filtrate was repeatedly partitioned with CH_2Cl_2 and H_2O . The organic soluble fraction was discarded, and the $\text{MeOH}/\text{H}_2\text{O}$ layer was concentrated on a rotary evaporator prior to lyophilization (Büchi). Then the mixture was diluted with distilled H_2O to a final MeOH concentration < 20% and lyophilized on a freeze-drier (Speedvac). The dried material was redissolved in a minimal amount of buffer A (0.05% TFA prepared in distilled H_2O). The solution was then passed through a filter by using a solid-phase filter (Sartorius) before purification using a preparative Phenomenex Jupiter C18 column (250 × 22 mm, 5 μm , 300 Å). Gradients of buffer A (0.05% aqueous TFA) and buffer B (90% CH_3CN , 0.05% TFA) were employed with a flow rate of 8 mL/min and a gradient of 1% buffer B per minute. Further purification was

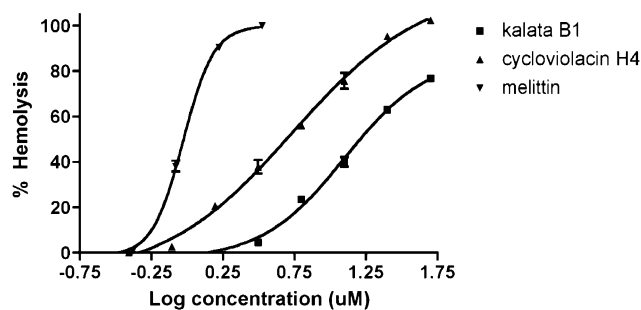


Figure 4. Hemolytic activities of melittin, cycloviolacin H4, and kalata B1. The HD_{50} values (and 95% confidence intervals) were calculated using Prism software to be 12.7 μM (11.0–14.6) for kalata B1, 5.5 μM (4.3–6.9) for cycloviolacin H4, and 0.94 μM (0.90–0.97) for melittin. Melittin is a well-known hemolytic agent that is used as a positive control. As a negative control, the cyclotide tricyclon A has been shown to have significantly lower activity than kalata B1, with a maximum activity of 2% hemolysis at concentrations up to 80 μM .²⁵

performed using semipreparative RP-HPLC on a Phenomenex Jupiter C18 column (250 × 10 mm, 5 μm , 300 Å) and using an analytical Phenomenex Jupiter C18 column (250 × 4.6 mm, 5 μm , 300 Å). The final purity was examined with analytical RP-HPLC on a Grom column (150 × 2 mm, 3 μm , equipped with a Security-guard column) with a flow rate of 300 $\mu\text{L}/\text{min}$.

Aminoethylation of Cysteines. The cyclotide cycloviolacin H4 (5 nmol) was reduced with 0.4 μmol of DTT in 200 μL of 0.25 M Tris-HCl, containing 1 mM EDTA and 8 M guanidine-HCl (pH 8.5, 37 °C) under N_2 . After 2 h, 20 μmol of bromoethylamine dissolved in 20 μL of 0.25 M Tris-HCl, containing 1 mM EDTA and 8 M guanidine-HCl (pH 8.5) was added. The reaction was incubated overnight in the dark

Table 3. Sequence Ions Observed in MS/MS Analysis of Cycloviolacin H4

trypsin	ion	m/z	ion	m/z	thermolysin	ion	m/z	ion	m/z
VWIPC*			y ₁	165.1	VCYNGIPCAESC			y ₁	122.1
330.68 ²⁺	b ₂	286.1	y ₂	262.1	629.77 ²⁺	b ₂	203.1	y ₂	209.1
M _r = 659.36	b ₃	399.2	y ₃	375.2	M _r = 1257.54	b ₃	366.2	y ₃	338.1
			y ₄	561.3		b ₄	480.2	y ₄	409.2
TVTALLGC*			y ₁	165.1		b ₅	537.2	y ₅	512.2
410.74 ²⁺	b ₂	201.1	y ₂	222.1		b ₆	650.3	y ₆	609.2
M _r = 819.48	b ₃	302.2	y ₃	335.2		b ₇	747.3	y ₇	722.3
	b ₄	373.2	y ₄	448.3		b ₈	850.3	y ₈	779.3
	b ₅	486.2	y ₅	519.3		b ₉	921.4	y ₉	893.4
	b ₆	599.3	y ₆	620.4		b ₁₀	1050.4		
			y ₇	719.4		b ₁₁	1137.5		
YNGIPC*AESC*			y ₁	165.1	NGIPCAESCVWIPCT			y ₁	120.1
571.74 ²⁺	b ₂	278.1	y ₂	252.1	796.85 ²⁺	b ₂	172.1	y ₂	223.1
M _r = 1141.48	b ₃	335.1	y ₃	381.1	M _r = 1591.70	b ₃	285.2	y ₃	320.1
	b ₄	448.2	y ₄	452.2		b ₄	382.2	y ₄	433.2
	b ₅	545.2	y ₅			b ₅		y ₅	619.3
	b ₆	691.3	y ₆	695.3		b ₆	556.2	y ₆	718.4
	b ₇	762.3	y ₇	808.3		b ₇	685.3	y ₇	
	b ₈	891.4	y ₈	865.4		b ₈	772.3	y ₈	908.5
	b ₉	978.4	y ₉	979.4		b ₉	875.4		
						b ₁₀	974.4		
						b ₁₁	1160.5		
						b ₁₂	1273.6		
SNNVC*YNGIPC*AESC*			y ₁	165.1	VCYNGIPCAESCVWIPCT			y ₁	120.1
568.25 ³⁺	b ₂	202.1	y ₂	252.1	979.41 ²⁺	b ₂	203.1	y ₂	223.1
M _r = 1701.75	b ₃	316.1	y ₃		M _r = 1956.82	b ₃	366.2	y ₃	320.1
	b ₄	415.2	y ₄	452.2		b ₄	480.2	y ₄	433.2
	b ₅		y ₅ ²⁺	299.6		b ₅	537.2	y ₅	619.3
	b ₆		y ₆	695.3		b ₆	650.3	y ₆	718.4
			y ₆ ²⁺	348.2		b ₇	747.4	y ₇	
	b ₇		y ₇	808.3		b ₈	850.4	y ₈	908.5
	b ₈	895.4	y ₈	865.4		b ₉	921.4	y ₉	1037.5
	b ₈ ²⁺	448.2				b ₁₀	1050.5		
	b ₉	1008.4	y ₉ ²⁺	490.2		b ₁₁	1137.5		
	b ₉ ²⁺	504.7				b ₁₂	1240.5		
	b ₁₀ ²⁺	553.2	y ₁₀			b ₁₃	1339.6		
			y ₁₁ ²⁺	644.7		b ₁₄	1525.7		
						b ₁₅	1638.7		

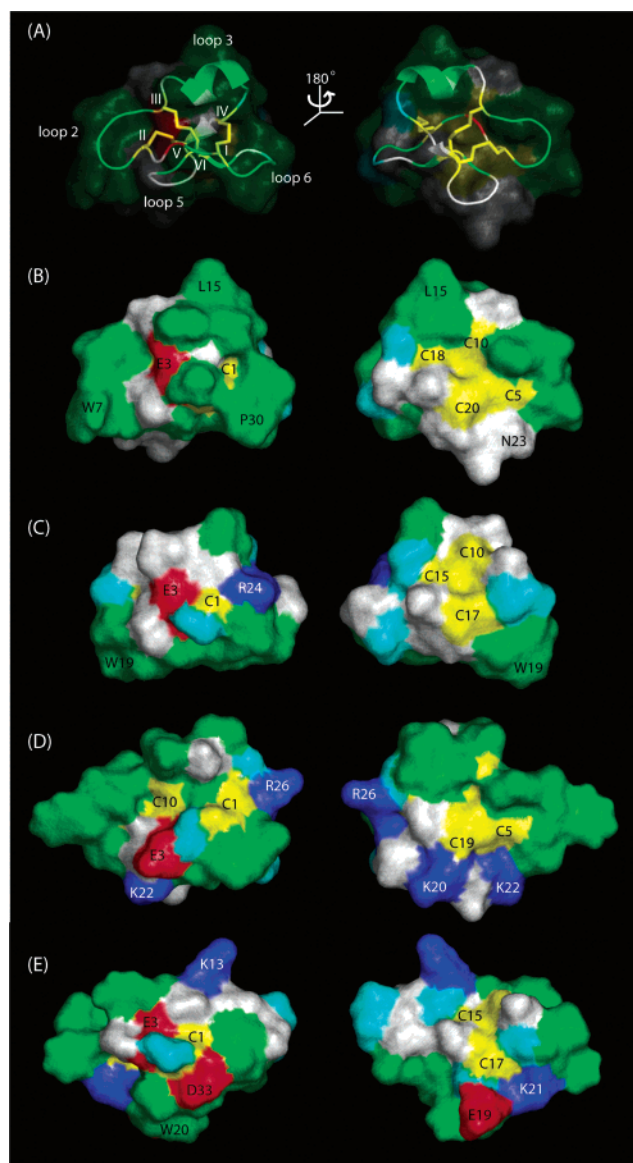


Figure 5. Surface representations of selected cyclotides. (A) Transparent surface on a ribbon diagram to illustrate the orientation of cycloviolacin H4. Surfaces of (B) cycloviolacin H4, (C) kalata B1, (D) circulin A, and (E) tricyclon A are shown. Hydrophobic residues (Ala, Leu, Ile, Pro, Trp, Phe, and Val) are green, polar residues (Asn, Ser, Thr, and Tyr) are white, basic residues (Arg and Lys) are blue, acidic residues (Asp and Glu) are red, glycine is cyan, and cysteines are yellow.

Table 4. Surface Properties and Charge Distribution of Cyclotides

	cycloviolacin H4	kalata B1	circulin A	tricyclon A
surface area (\AA^2) ^a	2333	2009	2551	2674
hydrophobic (%) ^b	67.8	45.8	55.6	43.8
polar (%) ^c	26.0	31.3	16.8	19.1
charged (%) ^d	1.6	5.9	21.1	23.3
net charge ^e	-1 (0, -1)	0 (+1, -1)	+2 (+3, -1)	-1 (+2, -3)

^a Calculated using MOLMOL.²⁴ ^b Includes Val, Pro, Leu, Ile, Trp, Tyr, Ala, Cys, Phe. ^c Includes Thr, Ser, Asn. ^d Includes Lys, Arg, Glu, Asp. ^e Net charge, with net positive and negative charge, shown in parentheses.

in a water bath at 37 °C under N₂, then terminated by injection onto RP-HPLC, eluted with a linear gradient of 0–80% buffer B in 80 min. The masses of collected fractions were confirmed by MS prior to lyophilization and storage at -20 °C.

Reduction of Cycloviolacin H4 and MALDI-MS Analysis. To 6 nmol of cycloviolacin H4 in 20 μL of 0.1 M NH_4HCO_3 (pH 8.0) was added 1 μL of 0.1 M TCEP, and the solution was incubated at 65 °C for 10 min. The reduction was confirmed by MALDI-TOF-MS after desalting using Ziptips (Millipore), which involved several washing steps followed by elution in 10 μL of 80% CH_3CN (0.5% formic acid). The desalted samples were mixed in a 1:1 ratio with matrix consisting of a saturated solution of α -cyano-4-hydroxycinnamic acid (CHCA) in 50% acetonitrile (0.5% formic acid).

Enzymatic Digestion and Nanospray MS/MS Sequencing. To the reduced peptide, trypsin, chymotrypsin, or a combination of EndoGluC and trypsin was added to give a final peptide-to-enzyme ratio of 50:1. The trypsin incubation was allowed to proceed for 1 h, the chymotrypsin digestion was allowed to proceed for 3 h, while for the combined digestion trypsin was added initially for 1 h followed by the addition of EndoGluC and a further 3 h incubation. The digestions were quenched by the addition of an equal volume of 0.5% formic acid and desalted using Ziptips (Millipore). Samples were stored at 4 °C prior to analysis. The fragments resulting from the digestion were examined first by MALDI-TOF-MS followed by nanospray MS/MS analysis on a QStar mass spectrometer. The MS/MS spectra were examined and sequenced based on the presence of both b- and y-series of ions present (N- and C-terminal fragments).

Homology Model of Cycloviolacin H4. The NMR structure of vhr1 (PDB ID 1VB8) was identified as a suitable template from a sequence similarity search on all cyclotide structures using standalone BLAST. Modeller 8v1,²⁸ a restraint-based structure generation program, was used to generate 100 models of cycloviolacin H4. The model with the lowest energy, according to Modeller 8v1, was selected and evaluated. The programs PROCHECK and MOLMOL were used to analyze and visualize the modeled structure.

Hemolytic Activity Assay. Peptides were dissolved in H₂O and serially diluted in phosphate-buffered saline (PBS) to give 20 mL test solutions in a 96-well U-bottomed microtiter plate (Nunc). Human type A red blood cells (RBCs) were washed with PBS and centrifuged at 4000 rpm for 60 s in a microcentrifuge several times until a clear supernatant was obtained. A 0.25% suspension of washed RBCs in PBS was added (100 μL) to the peptide solutions. The plate was incubated at room temperature for 1 h and centrifuged at 150 g for 5 min. Aliquots of 100 μL were transferred to a 96-well flat-bottomed microtiter plate (Falcon), and the absorbance was measured at 405 nm with an automatic Multiskan Ascent plate reader (LabSystems). The level of hemolysis was calculated as the percentage of maximum lysis (1% Triton X-100 control) after adjusting for minimum lysis (PBS control). Synthetic melittin (Sigma) was used for comparison.

Acknowledgment. This work was supported by a grant from the Australian Research Council (ARC). D.C. is an ARC Professional Fellow. B.C. acknowledges the Chinese Academy of Sciences for a visiting scholarship.

References and Notes

- (1) Craik, D. J.; Daly, N. L.; Bond, T.; Waine, C. *J. Mol. Biol.* **1999**, *294*, 1327–1336.
- (2) Saether, O.; Craik, D. J.; Campbell, I. D.; Sletten, K.; Juul, J.; Norman, D. G. *Biochemistry* **1995**, *34*, 4147–4158.
- (3) Daly, N. L.; Koltay, A.; Gustafson, K., R.; Boyd, M. R.; Casas-Finet, J. R.; Craik, D. J. *J. Mol. Biol.* **1999**, *285*, 333–345.
- (4) Rosengren, K. J.; Daly, N. L.; Plan, M. R.; Waine, C.; Craik, D. J. *J. Biol. Chem.* **2003**, *278*, 8606–8616.
- (5) Barry, D. G.; Daly, N. L.; Bokesch, H. R.; Gustafson, K. R.; Craik, D. J. *Structure (Cambridge, U.K.)* **2004**, *12*, 85–94.
- (6) Trabi, M.; Craik, D. J. *Plant Cell* **2004**, *16*, 2204–2216.
- (7) Chen, B.; Colgrave, M. L.; Daly, N. L.; Rosengren, K. J.; Gustafson, K. R.; Craik, D. J. *J. Biol. Chem.* **2005**, *280*, 22395–22405.
- (8) Gran, L. *Lloydia* **1973**, *36*, 207–208.
- (9) Daly, N. L.; Gustafson, K. R.; Craik, D. J. *FEBS Lett.* **2004**, *574*, 69–72.
- (10) Gustafson, K. R.; McKee, T. C.; Bokesch, H. R. *Curr. Protein Pept. Sci.* **2004**, *5*, 331–340.
- (11) Tam, J. P.; Lu, Y. A.; Yang, J. L.; Chiu, K. W. *Proc. Nat. Acad. Sci. U.S.A.* **1999**, *96*, 8913–8918.
- (12) Lindholm, P.; U., G.; S., J.; Claesson, P.; Gulbo, J.; Larsson, R.; Bohlin, L.; Backlund, A. *Mol. Cancer Ther.* **2002**, *1*, 365–369.
- (13) Witherup, K. M.; Bogusky, M. J.; Anderson, P. S.; Ramjit, H.; Ransom, R. W.; Wood, T.; Sardana, M. *J. Nat. Prod.* **1994**, *57*, 1619–1625.

- (14) Schöpke, T.; Hasan Agha, M. I.; Kraft, R.; Otto, A.; Hiller, K. *Sci. Pharm.* **1993**, *61*, 145–153.
- (15) Hernandez, J. F.; Gagnon, J.; Chiche, L.; Nguyen, T. M.; Andrieu, J. P.; Heitz, A.; Trinh Hong, T.; Pham, T. T.; Le Nguyen, D. *Biochemistry* **2000**, *39*, 5722–5730.
- (16) Jennings, C.; West, J.; Waine, C.; Craik, D.; Anderson, M. *Proc. Natl. Acad. Sci. U.S.A.* **2001**, *98*, 10614–10619.
- (17) Jennings, C. V.; Rosengren, K. J.; Daly, N. L.; Plan, M.; Stevens, J.; Scanlon, M. J.; Waine, C.; Norman, D. G.; Anderson, M. A.; Craik, D. J. *Biochemistry* **2005**, *44*, 851–860.
- (18) Basse, C. W. *Plant Physiol.* **2005**, *138*, 1774–1784.
- (19) Goransson, U.; Broussalis, A. M.; Claeson, P. *Anal. Biochem.* **2003**, *318*, 107–117.
- (20) Trabi, M.; Svargard, E.; Herrmann, A.; Goransson, U.; Claeson, P.; Craik, D. J.; Bohlin, L. *J. Nat. Prod.* **2004**, *67*, 806–810.
- (21) Craik, D. J.; Daly, N. L.; Mulvenna, J.; Plan, M. R.; Trabi, M. *Curr. Protein Pept. Sci.* **2004**, *5*, 297–315.
- (22) Barry, D. G.; Daly, N. L.; Clark, R. J.; Sando, L.; Craik, D. J. *Biochemistry* **2003**, *42*, 6688–6695.
- (23) Laskowski, R. A.; MacArthur, M. W.; Moss, D. S.; Thornton, J. M. *J. Appl. Crystallogr.* **1993**, *26*, 283–291.
- (24) Koradi, R.; Billeter, M.; Wüthrich, K. *J. Mol. Graph.* **1996**, *14*, 51–5, 29–32.
- (25) Mulvenna, J. P.; Sando, L.; Craik, D. J. *Structure (Cambridge, U.K.)* **2005**, *13*, 691–701.
- (26) Shai, Y. *Biochim. Biophys. Acta* **1999**, *1462*, 55–70.
- (27) Craik, D. J.; Simonsen, S.; Daly, N. L. *Curr. Opin. Drug Discuss. Dev.* **2002**, *5*, 251–260.
- (28) Sali, A.; Blundell, T. L. *J. Mol. Biol.* **1993**, *234*, 779–815.
- (29) Anders, J. C. *Advances in Amino Acid Analysis. Biopharm Eur.* **2002**, 32–39.

NP050317I